

Quantum Tunneling of Vortices in Two-Dimensional Condensates

Assa Auerbach¹, Daniel P. Arovas² and Sankalpa Ghosh¹

¹*Physics Department, Technion, Haifa, 32000 Israel*

²*Department of Physics, University of California at San Diego, La Jolla, CA 92093*

(Dated: May 24, 2019)

We investigate quantum mechanical tunneling of vortices in two-dimensional superfluids and superconductors. In the weak pinning limit, tunneling rates can be expressed directly in terms of wavefunction overlaps. We compute the Bogoliubov, and Bogoliubov-de Gennes vortex ground states for the Bose-Einstein condensate (BEC) and BCS superconductor respectively, in the planar and spherical geometries. We find an *orthogonality catastrophe* in the overlaps of vortex ground states, centered at separate pinning sites. The theoretical implication is that vortices self-trap, and cannot form coherent Bloch waves. Experimentally, vortex tunneling in a low-density BEC yields a power law dissipative response. We calculate this power by maximizing the overlap between a relaxed vortex at one pinning site, and a deformed (excited) vortex on another, subject to conservation of energy. We obtain the non linear magneto-resistance of a low superfluid density 'bosonic' superconductor, which might be realized in underdoped cuprate films, Josephson junction arrays, or cold atoms BEC.

PACS numbers: 03.75.Lm, 66.35.+a

I. INTRODUCTION

Vortices play an important role in equilibrium and transport properties of two dimensional systems with two-component order parameters. For example, the Berezinskii-Kosterlitz-Thouless transition in planar magnets is governed by vortex-antivortex unbinding [1]. Mass and charge transport in superfluids, Bose-Einstein condensates (BEC), and superconductors are governed by vortex mobility [2, 3].

Theoretically, vortices have often been usefully treated as point particles, with vortex centers defined as collective coordinates [3, 4]. Their effective interactions are generated by tracing over microscopic degrees of freedom (bosons, electrons, spins, *etc.*). At higher temperatures, a classical particulate theory for vortex motion is applicable: vortex mobility is dominated by thermally activated hopping or classical diffusion by relaxation of core excitations [5, 6, 7, 8, 9]. At lower temperatures, vortices get pinned and their mobility is rapidly suppressed. Nevertheless, quantum phase fluctuations may, in principle, admit tunneling of vortices under the barriers [10]. Quantum tunneling may be detected as a finite angular momentum relaxation rate in the zero temperature limit, or in disordered superconducting films, a finite resistivity or magnetization relaxation rate [11, 12].

However the task of quantizing the vortex as a point particle in order to derive its dynamics or wavefunction is nontrivial [13], as we discuss in Section VI. Naïvely, since the motion of a vortex results in the accrual of a geometric phase $2\pi N_{\text{enc}}$, where N_{enc} is the number of bosons encircled by the path of the vortex. For a single vortex, this reasoning leads to an effective Lagrangian $L_0 = \pm 2\pi\hbar n_0 X\dot{Y} - V_{\text{eff}}(X, Y)$, where n_0 is the average condensate density, and where V_{eff} is an effective potential in terms of the vortex coordinates. The vortex thus acts as a point particle with zero mass in a uniform ex-

ternal magnetic field. However, when other degrees of freedom are accounted for (*e.g.* condensate phase fluctuations, vortex core excitations, *etc.*), additional terms are generated in the effective vortex Lagrangian, leading to a frequency-dependent effective vortex mass, quantum dissipation, *etc.*. The impact of these gapless, anharmonic excitations on the physics of vortex tunneling must be considered in any complete theory.

In this paper we use a different approach which avoids some of these difficult issues, by using many-body vortex wavefunctions. This allows us to incorporate, in principle, the strong correlations present in established examples of vortex wavefunctions, and to deduce the following general results:

(i) In the presence of two weak pinning sites (labelled 1 and 2) of strength \bar{V} separated by a distance d , the vortex coherent tunneling rate is related to the overlap between single pinning site ground states $|\Phi_1\rangle, |\Phi_2\rangle$:

$$\nu_c(d) = \frac{\bar{V}}{\hbar} |\langle \Phi_1 | \Phi_2 \rangle|. \quad (1)$$

This overlap is computed for the interacting Bose-Einstein condensate (BEC) and for the *s*-wave Bardeen-Cooper-Schrieffer (BCS) superconductor. Expressions similar to (1) for vortex tunneling rates, have been previously used for specific wavefunctions [14, 15, 16].

(ii) We show that for general condensates, Eq. (1) suffers an *orthogonality catastrophe* in the thermodynamic limit

$$\log(\nu_c) \sim -\frac{\pi}{2} n_{\text{eff}} d^2 \log(R/\xi), \quad (2)$$

where R is the system's size, ξ is a short-distance cutoff, and the effective overlap density n_{eff} depends on the far field properties of the condensate. We calculate n_{eff} explicitly for non interacting boson coherent states, Bogoliubov corrected BEC wavefunctions and the BCS superconductor.

Thus we find that vortex tunneling belongs to the celebrated class of Anderson's *orthogonality catastrophes* [17, 18, 19], which include the X-ray edge absorption, the Kondo effect and dissipative quantum tunneling.

This orthogonality catastrophe follows from the slow decay of the condensate phase adjustments at large distances from the cores. Dynamical calculations have also found a logarithmic divergence of the vortex effective mass at low frequencies [20, 21, 22], but mass renormalization in itself does not suppress tunneling since the mass is to be evaluated at a finite tunneling time scale. We shall elaborate on this subtle point in the Section VI.

The primary theoretical implication of Eq.(2), is that vortices in superfluid phase are in a sense 'classical': They spontaneously self-trap, and break translational symmetry, and do not lend themselves to forming Bloch waves. An experimental implication of the logarithmic divergence, is an expected power law dependence of the *incoherent* tunneling rate on the bias current. We propose to detect vortex tunneling in low superfluid density systems by observing this power law.

The paper is organized as follows: In Section II the vortex tunneling rate for the symmetric (coherent) and biased (incoherent) cases is derived in terms of non-orthogonal ground state overlaps. For pedagogical illustration, we demonstrate that the non interacting mean field (MF) vortex overlap exhibits the orthogonality catastrophe (2) where n_{eff} is the condensate density. This result is modified however in Section III, where the overlap is calculated for an interacting BEC within Bogoliubov theory. Remarkably, the logarithmic divergence of the leading order (in condensate density) overlap is exactly cancelled by Bogoliubov corrections. It is however replaced by another overlap catastrophe arising from the fluctuation determinant – in effect one replaces n_{eff} in Eq. (2) by $4\delta n$, where δn is the density change due to the Bogoliubov fluctuations.

In Section IV we discuss the case of an *s*-wave BCS superconductor vortex. Bogoliubov-de Gennes theory provides us with the second quantized wavefunctions, whose overlaps are determinants. Here, the logarithmic divergence in (2), is controlled by $n_{\text{eff}} = n_e \Delta / 8\varepsilon_F$, where n_e is the electron density, Δ the BCS gap, and ε_F the Fermi energy. At weak coupling $\Delta/\varepsilon_F \ll 1$, the core contribution to the exponent is very large (even though it doesn't diverge with R), and this in effect suppresses vortex tunneling at distances $d > 2\pi/k_F$. Absence of tunneling, as defined here, does not preclude vortex creep by intracore states scattering [6, 7, 8, 10].

In Section V we use a variational calculation of the vortex tunneling rate to connect the logarithmic divergence found in Section to an expected asymptotic power law $V \propto I^\alpha$ response of the dissipative transport equation at zero temperature. We that non linear magnetoresistance might be observable in cuprate superconducting thin films.

In Section VI we discuss an open theoretical issue: the apparent absence of orthogonality catastrophe effects

within the linearized quantum electrodynamics approach to vortex dynamics. We conclude in Section VII with a and a summary of the results and their experimental implications. Technical details, such as explicit calculations of overlap exponents, setting up Bogoliubov equations for BEC and BCS vortices on the sphere, and a variational calculation of the incoherent vortex tunneling rate, are relegated to the appendices.

II. VORTEX TUNNELING

A. Coherent Tunneling

As a first step, we calculate the *coherent* vortex tunneling rate between two weak, and symmetrically situated, pinning sites. We follow the method of Heitler and London [23], using non-orthogonal ground states of partial Hamiltonians. The main purpose here is to formulate the connection between the tunneling rate and the vortex wavefunction overlap.

Consider a many-body interacting Hamiltonian \mathcal{H}_0 describing an interacting Bose fluid or a Fermi fluid with a pairing instability. In addition, consider two identical weak (relative to energy scales of \mathcal{H}_0) localized pinning potentials at \mathbf{x}_1 and at \mathbf{x}_2 , so that the full Hamiltonian is $\mathcal{H} = \mathcal{H}_0 + V_1 + V_2$, where $V_i = \lambda n(\mathbf{x}_i)$. The pinning potentials are repulsive for bosons ($\lambda > 0$) and are hence attractive for the vortices. The separation between the pins is $d = |\mathbf{x}_2 - \mathbf{x}_1|$. We assume for this exercise that a reflection symmetry exists in \mathcal{H} about a mirror plane between the pinning sites. The ground states $|\Psi_i^0\rangle$ of the two *partial* Hamiltonians satisfy $(\mathcal{H}_0 + V_i)|\Psi_i^0\rangle = E_0|\Psi_i^0\rangle$. Thus we can use the symmetric and antisymmetric superpositions $|\Psi_1^0\rangle \pm |\Psi_2^0\rangle$ as a basis for the ground states for the two symmetry sectors, within lowest order degenerate perturbation theory. Their corresponding energies are given by solving

$$\det_{ij} \langle \Psi_i^0 | \mathcal{H} - E | \Psi_j^0 \rangle = 0. \quad (3)$$

The coherent tunneling rate is given by $\nu_c = (E_+ - E_-)/2\hbar$. To first order in V_i , we obtain

$$\begin{aligned} \nu_c &= \hbar^{-1} \left| \langle \Psi_1^0 | V_2 | \Psi_1^0 \rangle \cdot \langle \Psi_1^0 | \Psi_2^0 \rangle - \langle \Psi_1^0 | V_2 | \Psi_2^0 \rangle \right| \\ &\approx \frac{\bar{V}}{\hbar} \left| \langle \Psi_1^0 | \Psi_2^0 \rangle \right|, \end{aligned} \quad (4)$$

where $\bar{V} \equiv \langle \Psi_1^0 | V_2 | \Psi_1^0 \rangle \approx \lambda n_1(\mathbf{x}_2)$. We neglect the term proportional to $\langle \Psi_1^0 | V_2 | \Psi_2^0 \rangle$ since it depends on the density at the vortex center, which is assumed here to be small.

Thus, Eq. (4) establishes that the pinning potential supplies the 'attempt rate' of the tunneling, and the vortex wavefunctions' overlap governs its decrease with separation d . In the following, we shall find that both for the BEC and BCS cases, an overlap catastrophe results

whereby $\lim_{R \rightarrow \infty} \nu_c(d, R) = 0$. This dynamic localization prevents the vortices from forming extended coherent superpositions (*e.g.* Bloch waves) in the case of a lattice of pinning sites. It also produces non-ohmic power law behavior of the dissipative transport, as we shall subsequently explore.

B. Incoherent Tunneling

The orthogonality catastrophe notwithstanding, a vortex can still tunnel *incoherently* between pinning sites under an energy bias, by an incoherent decay process. Consider the previous case, but now let us include the excited states $|\Psi_i^\alpha\rangle$ in the analysis. The energy dissipated during the tunneling process is set to E_{bias} . This can be externally controlled, for a given distribution of pins, through a uniform supercurrent. We now write

$$\begin{aligned} (\mathcal{H}_0 + V_1)|\Psi_1^0\rangle &= E_0|\Psi_1^0\rangle \\ (\mathcal{H}_0 + V_2)|\Psi_2^\alpha\rangle &= (E_\alpha + E_{\text{bias}})|\Psi_2^\alpha\rangle. \end{aligned} \quad (5)$$

In the low energy subspace $|\Psi_1^0\rangle \otimes |\Psi_2^\alpha\rangle$ the resolvent is given by

$$G^{-1} \equiv \begin{pmatrix} \langle \Psi_1^0 | \mathcal{H} - E | \Psi_1^0 \rangle & \dots & \langle \Psi_1^0 | \mathcal{H} - E | \Psi_2^\alpha \rangle \\ \vdots & \ddots & \vdots \\ \langle \Psi_2^{\alpha'} | \mathcal{H} - E | \Psi_1^0 \rangle & \dots & \langle \Psi_2^{\alpha'} | \mathcal{H} - E | \Psi_2^\alpha \rangle \end{pmatrix}. \quad (6)$$

We are interested in the decay rate of the vortex state $|\Psi_1^0\rangle$, which is given by an imaginary contribution to the self energy at the lowest pole of $G_{11}(E) = \langle 1 | G^{-1} | 1 \rangle$. Using the matrix inversion formula,

$$\begin{aligned} \langle 1 | G^{-1} | 1 \rangle &= E_0 + \bar{V} - E \\ &- \sum_{\alpha} \frac{\langle \Psi_1^0 | \mathcal{H} - E | \Psi_2^\alpha \rangle^2}{E_\alpha + \bar{V} - E_{\text{bias}} - E + i0^+}. \end{aligned} \quad (7)$$

To lowest order in the overlap, we set the real part of the pole to $\text{Re } E = E_0 + \bar{V}$, and we obtain the tunneling rate $\gamma = \text{Im } E/\hbar$,

$$\gamma = \frac{\pi}{\hbar} \bar{V}^2 \sum_{\alpha} |\langle \Psi_1^0 | \Psi_2^\alpha \rangle|^2 \delta(E_{\text{bias}} - E_\alpha + E_0). \quad (8)$$

Here, as in Eq. (4), we have made simplifying assumptions on the pinning potential, such as ignoring $\langle \Psi_1^0 | V_2 | \Psi_2^\alpha \rangle$. We also assume that $\langle \Psi_2^\alpha | V_1 | \Psi_2^{\alpha'} \rangle = \bar{V} \delta_{\alpha, \alpha'}$, which could slightly modify the pre-exponential factors.

Expression (8) relates the decay rate directly to the wavefunction overlap, as in the coherent case. For a finite E_{bias} , energy conservation requires the final vortex to be excited. Integration over final states is dominated by *distorted* configurations with maximal overlaps, constrained to have $E_\alpha - E_0 = E_{\text{bias}}$. The decay rate can thus be estimated variationally, as we shall do further on below.

C. Vortex Coherent State Overlap

The boson coherent state $|\varphi\rangle$, with $\varphi = \sqrt{n} e^{i\phi}$ a complex scalar field, is defined by

$$|\varphi\rangle = \exp \int d^2x \left(\varphi(\mathbf{x}) \psi^\dagger(\mathbf{x}) - \varphi^*(\mathbf{x}) \psi(\mathbf{x}) \right) |0\rangle. \quad (9)$$

The overlap exponent between two translated vortex

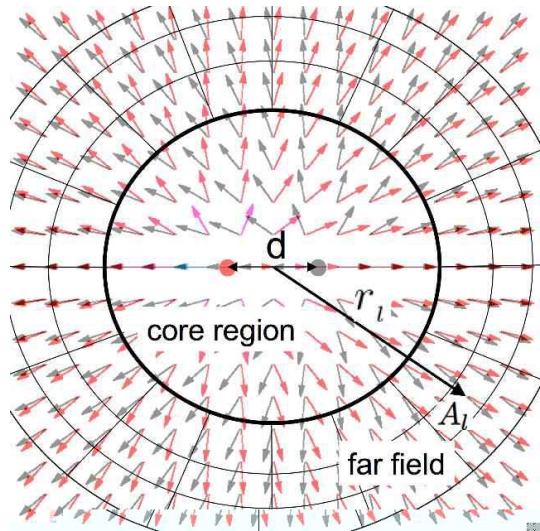


FIG. 1: Overlap of two vortex coherent states as described by Eq. (10). Black (red) arrows are vector representation of φ_1 (φ_2). For asymptotic calculations of BEC and BCS cases, see Eqs.(33,48), the far field region is divided into uniform phase blocks labelled by l at distances r_l and areas A_l .

coherent states (9), centered at $\mathbf{X} = \pm \frac{1}{2} \mathbf{d}$ is then $|\langle \varphi_1 | \varphi_2 \rangle| = \exp(-W)$, with

$$W = \int d^2x \left[\frac{1}{2} (|\varphi_1|^2 + |\varphi_2|^2) - \text{Re} \varphi_1^* \varphi_2 \right].$$

It is easy to evaluate the far field integral (away from the core), where $n_i(\mathbf{x}) \simeq n_0$. In this case, $\varphi \sim \sqrt{n_0} \exp(i\phi)$, where ϕ is the angle function relative to the vortex center (see Fig. 1). The overlap exponent is then found to be

$$\begin{aligned} W_{\text{far}}(d) &= n_0 \int_{r_0}^R d^2x \left[1 - \cos(\phi_1 - \phi_2) \right] \\ &\approx \frac{1}{2} n_0 \int_{r_0}^R d^2x \left(\frac{\mathbf{d} \cdot \nabla \phi}{r} \right)^2 \\ &= \frac{1}{2} \pi n_0 d^2 \ln(R/r_0), \end{aligned} \quad (10)$$

where r_0 can be chosen to be the larger of ξ and d . This calculation was first presented by Sonin [14], in the context of vortex tunneling using a noninteracting (product) condensate wavefunction. Eq.(10) agrees with Eq.(2)

with $n_{\text{eff}} = n_0$. It is worthwhile showing the exact numerical result for two cases: (i) a coreless vortex $n = n_0$ on a disk of radius R (worked out in Appendix A)

$$W_{\text{disk}}(d) = \frac{1}{2}\pi n_0 d^2 \ln \left(\frac{C_d R}{d} \right), \quad C_d = 2.01454 \quad (11)$$

and (ii) an antipodal vortex-antivortex pair on a sphere of radius R , with finite core size ξ , depicted in Fig.2, for which the first vortex is

$$\varphi(\theta, \phi) \approx \frac{\sin \theta \sqrt{n_0}}{\sqrt{\sin^2 \theta + (\xi/R)^2}} e^{i\phi}, \quad (12)$$

which is an approximate solution to the classical Gross-Pitaevski (nonlinear Schrödinger) equation. The second vortex has its poles axis rotated by angle d/R . Here we take half of the overlap exponent to extract the single vortex result:

$$W_{\text{sphere}}(d) = \frac{1}{2}\pi n_0 d^2 \ln \left(\frac{C_s R}{\sqrt{d^2 + \xi^2}} \right), \quad (13)$$

with $C_s = 3.15 \pm 0.1$, and where

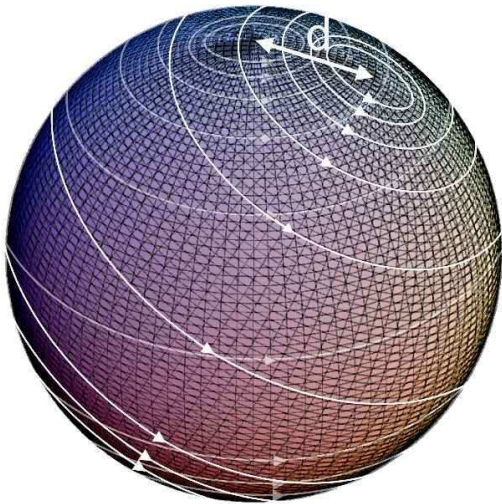


FIG. 2: Overlap of two antipodal vortex-antivortex pair states, relatively rotated by a angle d/R on a sphere. White circles depict directions of circulating currents described by the classical fields $\varphi_i, i = 1, 2$.

The orthogonality catastrophe, seen explicitly in (10,11,13), arises from the slow decay of the phase difference due to the vortex motion at large distances. For configurations which include well separated vortices (and anti-vortices), the results (10,11) still hold for the motion of a single vortex, since the phases from all stationary vortices simply cancel in the product $\varphi_1^* \varphi_2$.

This discussion has served only as a pedagogical example. Recall, however, that non interacting bosons do

not support stable vortices as their coherence length is infinite! In the following section on the interacting BEC, we find that the order n_0 term in W is exactly cancelled by the Bogoliubov corrections, and that the divergence reappears at the next order in the dimensionless parameter $1/(4\pi n_0 \xi^2)$.

III. VORTEX OVERLAP IN THE BEC

A. Mean field theory of interacting bosons

Let us consider a two-dimensional boson liquid with short range interactions, described by

$$\mathcal{H} = \int d^2x \left\{ \psi^\dagger K(\mathbf{A}) \psi + V(\mathbf{x}) \psi^\dagger \psi + \frac{g}{2} \psi^\dagger \psi^\dagger \psi \psi \right\}, \quad (14)$$

$\psi^\dagger(\mathbf{x})$ creates a boson of mass m and charge q at position \mathbf{x} ; μ is the chemical potential. The single particle potential $V(\mathbf{x})$ includes confining and vortex pinning contributions. The kinetic operator is

$$K(\mathbf{A}) = \frac{1}{2m} \left(\frac{\hbar}{i} \nabla + \frac{q}{c} \mathbf{A} \right)^2, \quad (15)$$

and \mathbf{A} is a vector potential. In the case of bosons of charge q in a magnetic field $\mathbf{B} = B \hat{z}$ and subject to a rotation $\boldsymbol{\omega} = \omega_{\text{rot}} \hat{z}$, the vector potential is $\mathbf{A} = (\frac{1}{2}B + mcq^{-1}\omega_{\text{rot}})\hat{z} \times \mathbf{x}$, and the single particle potential is shifted by $\Delta V(\mathbf{x}) = (\omega_{\text{rot}}/2c)(qB + mc\omega_{\text{rot}})\mathbf{x}^2$.

If the system is a uniform droplet of bulk density n_0 , the chemical potential gets pinned at $\mu = gn_0$. The important parameters of the condensate are the phonon (phason) velocity is $c_s = \sqrt{gn_0/m}$, and the coherence length is $\xi = \hbar/mc$.

We use boson coherent states (9) to set up a semiclassical expansion of the partition function,

$$\begin{aligned} \mathcal{Z} &= \int \mathcal{D}[\varphi, \varphi^*] \exp \left\{ \int_0^{\hbar\beta} d\tau \int d^2x (i\varphi^* \partial_\tau \varphi - \mathcal{H}[\varphi^*, \varphi]) \right\} \\ &\approx \exp(-\beta E_{MF}[\tilde{\varphi}]) \int \mathcal{D}[\eta, \eta^*] e^{-\mathcal{L}^{(2)}[\eta^*, \eta] + \mathcal{O}(\eta^3)} \end{aligned} \quad (16)$$

The first exponential is the classical (mean field) energy, and the remaining path integral is over the fluctuation field $\eta = \varphi - \tilde{\varphi}$.

The classical field $\tilde{\varphi}$ minimizes the variational energy $\langle \varphi | \mathcal{H} | \varphi \rangle$. It solves the Gross-Pitaevskii (GP) equation [24, 25],

$$\left(K(\mathbf{A}) + V - \mu + g|\tilde{\varphi}(\mathbf{x})|^2 \right) \tilde{\varphi}(\mathbf{x}) = 0, \quad (17)$$

With a weak pinning potential at the origin, and an external magnetic field or rotation [26], a stable vortex solution can be found, whose approximate analytic form is [27],

$$\tilde{\varphi} \approx \frac{\sqrt{n_0} r e^{i\phi}}{\sqrt{r^2 + \xi^2}}, \quad (18)$$

where (r, ϕ) are the polar coordinates of the vortex center. For numerical evaluation of the fluctuation spectrum, the trial solution (18) must be improved upon by iterating Eq. (17).

B. Bogoliubov fluctuations

The fluctuations η in (16), are governed by the harmonic action

$$S^{(2)} = \frac{1}{2} \int d\tau \int d^2x (\eta^* \eta) \left[iJ\partial_\tau - H^{(2)} \right] \begin{pmatrix} \eta \\ \eta^* \end{pmatrix}, \quad (19)$$

where

$$J \equiv \begin{pmatrix} 1 & 0 \\ 0 & -1 \end{pmatrix}, \quad H^{(2)} = \begin{pmatrix} H_0 & g\tilde{\varphi}^2 \\ g\tilde{\varphi}^{*2} & H_0^* \end{pmatrix}, \quad (20)$$

and $H_0 = K(\mathbf{A}) + 2g|\tilde{\varphi}(\mathbf{x})|^2 - \mu$.

The Hamiltonian $H^{(2)}$ is diagonalized by the canonical transformation,

$$S = \begin{pmatrix} U & V^* \\ V & U^* \end{pmatrix}, \quad S^\dagger H^{(2)} S = \begin{pmatrix} \hat{E} & 0 \\ 0 & \hat{E} \end{pmatrix}, \quad (21)$$

with

$$S^\dagger \hat{J} S = \hat{J} = S \hat{J} S^\dagger. \quad (22)$$

Here $\hat{E} = \delta_{nn'} E_n$ is the Bogoliubov spectrum [28]. The spectrum and eigenoperators are explicitly determined by solving the differential equations,

$$\begin{aligned} H_0 U_n(\mathbf{x}) + g\tilde{\varphi}^2 V_n(\mathbf{x}) &= +E_n U_n(\mathbf{x}) \\ g\tilde{\varphi}^{*2} U_n(\mathbf{x}) + H_0^* V_n(\mathbf{x}) &= -E_n V_n(\mathbf{x}), \end{aligned} \quad (23)$$

In Fig. 3, the numerical fluctuation spectrum about a vortex pair configuration on a sphere is plotted as a function of angular momentum.

Eq. (17) has a zero mode [29] ($E_n = 0$) corresponding to a global U(1) phase transformation $\phi \rightarrow \phi + \delta$, given by

$$\begin{aligned} U_0(\mathbf{x}) &= A\tilde{\varphi}(\mathbf{x}) & , & & V_0(\mathbf{x}) &= A^*\tilde{\varphi}^*(\mathbf{x}) \\ \int d^2x (|U_0|^2 - |V_0|^2) &= & 0. \end{aligned} \quad (24)$$

This (unnormalizable) zero mode, which enforces charge conservation, is henceforth excluded from our numerical spectra.

The Bogoliubov eigenoperators (quasiparticles) are given by

$$a_n = \int d^2x \left(U_n^*(\mathbf{x}) \eta(\mathbf{x}) - V_n^*(\mathbf{x}) \eta^*(\mathbf{x}) \right). \quad (25)$$

The Bogoliubov corrected ground state $|\Phi_0\rangle$ is the a -vacuum, and thus satisfies $a_n|\Phi_0\rangle = 0$. This may be

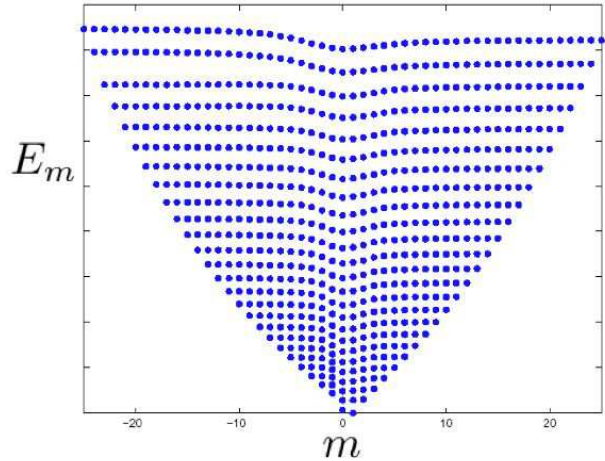


FIG. 3: The exact Bogoliubov spectrum for a vortex pair configuration on the sphere, as a function of azimuthal quantum number m . The relevant parameters are $\xi/R = 0.1$, and a stabilizing rotation frequency of $\omega_{\text{rot}} = 1.875 \hbar/mR^2$. Note the non-degenerate zero mode at $m = 1$. Note the vortices induced distortion of the spectrum around $m \approx 0$ in a broad energy range.

written in terms of the original bosons as

$$|\Phi_0\rangle = \mathcal{N} \exp\left(\frac{1}{2}\psi^\dagger Q \psi^\dagger\right) \exp(f\psi^\dagger) |0\rangle \quad (26)$$

$$f(\mathbf{x}) \equiv \tilde{\varphi}(\mathbf{x}) - \int d^2x' \tilde{\varphi}^*(\mathbf{x}') Q(\mathbf{x}', \mathbf{x}) \quad (27)$$

Integration over coordinates is implied in (26), and the normalization factor is $\mathcal{N} = \langle \Phi_0 | \Phi_0 \rangle^{-1/2}$. The pair operator Q is

$$Q(\mathbf{x}, \mathbf{x}') = \langle \mathbf{x} | (U^\dagger)^{-1} V^\dagger | \mathbf{x}' \rangle = Q(\mathbf{x}', \mathbf{x}), \quad (28)$$

where elimination of the zero mode (24) in U and V is implicitly assumed. To visualize the Bogoliubov fluctuations near a vortex, we plot in Figure (4) the tunneling density of states as defined by

$$T(E, \mathbf{x}) = \pi \sum_n |V_n(\mathbf{x})|^2 \delta(E - E_n), \quad (29)$$

which might prove interesting for inelastic scattering experiments of rotating condensates [30].

C. Uniform Condensate

In a large area, asymptotically far away from the vortex core, we can solve the Bogoliubov equations using a constant order parameter, $\tilde{\varphi} = \sqrt{n_0} e^{i\phi}$. $H^{(2)}$ is diagonal in Fourier space, and the matrix Q is given by

$$Q_{\mathbf{k}, \mathbf{k}'} = -\frac{e^{2i\phi}}{\mu} (\varepsilon_{\mathbf{k}} - \mu - E(\varepsilon_{\mathbf{k}})) \delta_{\mathbf{k}, \mathbf{k}'} \quad (30)$$

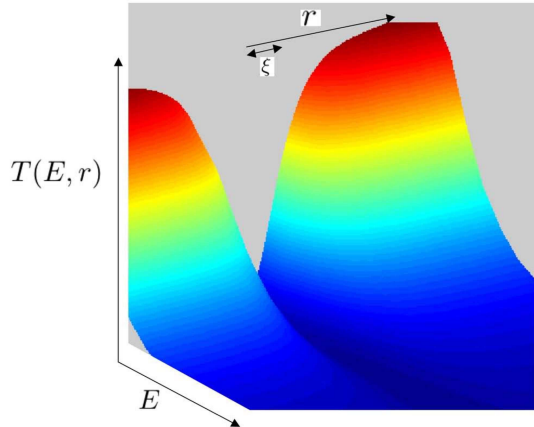


FIG. 4: The Bogoliubov tunneling density of states of a BEC vortex (in arbitrary units) as a function of excitation energy E and radial distance from the vortex center r . ξ is the coherence length.

where $\varepsilon_{\mathbf{k}} = \hbar^2 \mathbf{k}^2 / 2m$ and $E(\varepsilon) = \sqrt{\varepsilon^2 + 2\mu\varepsilon}$. The Bogoliubov fluctuations lead to an increase in the density, with

$$\delta n = \langle \Phi_0 | \eta^\dagger \eta | \phi_0 \rangle = \frac{1}{4\pi\xi^2}. \quad (31)$$

The dimensionless parameter which controls the higher order terms in the saddle point expansion of Eq. (16), is then $\delta n/n_0 = 1/(4\pi n_0 \xi^2)$, which serves as an effective 'quantum disorder' coupling constant. A quantum phase transition into another zero temperature phase (*e.g.* a solid) may be expected when $\delta n \gtrsim n_0$. Here we shall not explore the strong coupling regime.

D. Vortex States

In Fig. (5) we plot the numerical value of the fluctuation density as a function of radial direction from the vortex core, as calculated from Eqs.(23). δn achieves its asymptotic value (31) at distances much larger than the coherence length ξ .

We next compute the overlap of a vortex state with a displaced vortex. For two vortex states (27) centered at \mathbf{X}_i , $i=1,2$. the operators $Q_i(\mathbf{x}, \mathbf{x}')$ are distinct and not translationally invariant. The magnitude of the wavefunction overlap for Bogoliubov-corrected vortex states

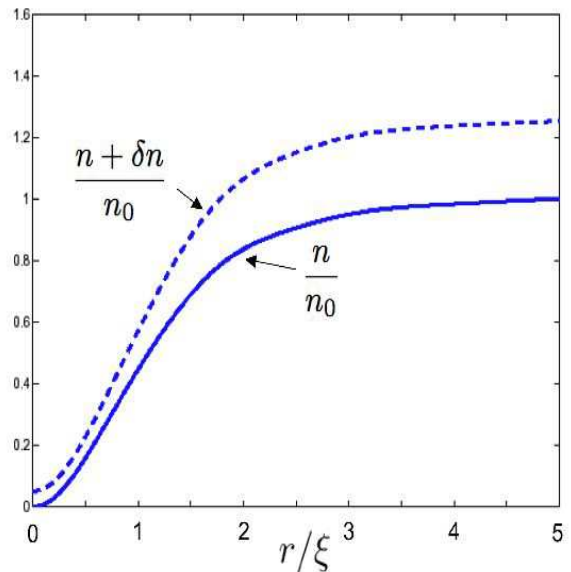


FIG. 5: The mean field condensate density profile $n(r)$ corrected by the Bogoliubov fluctuations density $\delta n(r)$ as a function of radial distance r from the vortex center. n_0 is the far field asymptotic density.

is

$$\begin{aligned} |\langle \Phi_1 | \Phi_2 \rangle| &= \exp(-W^0 - W^1) \\ W^0 &= W_{12}^0 - W_{11}^0 \quad , \quad W^1 = -\ln \left| \frac{D_{12}}{D_{11}} \right| \\ W_{ij}^0 &= \frac{1}{2} (f_i^* f_j) \begin{pmatrix} 1 & -Q_j \\ -Q_i^* & 1 \end{pmatrix}^{-1} \begin{pmatrix} f_j \\ f_i^* \end{pmatrix} \\ D_{ij} &= \det^{-1/2} (1 - Q_i^* Q_j) . \end{aligned} \quad (32)$$

We note that the leading order W^0 is proportional to the condensate density n_0 , while the fluctuation correction W^1 depends on d, ξ, R , but not on n_0 . Thus it is higher order in the small Bogoliubov parameter $\delta n/n_0$.

We now show that in contrast to the coherent state overlap result (10), there is no logarithmic divergence, to leading order, in the exponent $W^0(d, R)$. This can be shown analytically by separating contributions of the core and the far field regions, as depicted in Fig. 1,

$$W^0 \sim \int_{\text{core}} d^2x w_{\text{core}}(\mathbf{x}) + \sum_l A_l w_{\text{far}}(\mathbf{x}_l) . \quad (33)$$

The far field integral is approximated by a sum over constant phase domains, at radii $r_l \gg \xi$, and of areas $A_l \ll r_l^2$, corresponding to the condensate field $\varphi_{i,l} = \sqrt{n_0} \exp(i\phi_{i,l})$. We use the uniform solutions (30) in each such domain, assuming that the block sizes are

large enough: $A_x \gg \xi^2$. Thus,

$$\begin{aligned} Q_{i,l} &= -\frac{e^{2i\phi_{i,l}}}{A_l} \sum_{\mathbf{k}} Q_{\mathbf{k}} e^{i\mathbf{k}\cdot(\mathbf{x}-\mathbf{x}')} \\ &= -e^{i2\phi_{i,l}} \left(\delta(\mathbf{x}-\mathbf{x}') + \mathcal{O}(\xi/r_l) \right), \end{aligned} \quad (34)$$

which, by (27), yields in each block l , and vortex config-

urations $i = 1, 2$, the constant functions

$$\begin{aligned} f_{i,l}(\mathbf{x}) &= \sqrt{n_0} \left(e^{i\phi_{i,l}} - e^{-i\phi_{i,l}} \int_l d^2x' Q_{i,l}(\mathbf{x}, \mathbf{x}') \right) \\ &= 2\sqrt{n_0} e^{i\phi_{i,l}} + \mathcal{O}(\xi/R). \end{aligned} \quad (35)$$

Using (32) we obtain to zeroth order in ξ/r_l the result

$$w_{\text{far}}(\mathbf{x}_l) \simeq n_0 \text{Re} \left\{ \left(e^{-i\phi_1} e^{i\phi_2} \frac{\begin{pmatrix} 1 & -e^{i2\phi_2} \\ -e^{-i2\phi_1} & 1 \end{pmatrix}}{1 - e^{i2(\phi_2-\phi_1)}} \begin{pmatrix} e^{i\phi_2} \\ e^{-i\phi_1} \end{pmatrix} - (\phi_2 \leftrightarrow \phi_1) \right) \right\} = 4n_0 \text{Re} \left(\frac{e^{i(\phi_2-\phi_1)}}{1 + e^{i(\phi_2-\phi_1)}} - \frac{1}{2} \right) = 0, \quad (36)$$

where we have suppressed the block index l . Unlike in the coherent states overlap exponent which exhibits a logarithmic divergence (10), W^0 is perfectly finite in the large system limit:

$$\sum_l A_l w_l^{\text{far}} = \int_{r_0}^{\infty} d^2r (\mathbf{d} \cdot \nabla \phi)^2 \times \mathcal{O}(\xi/r) < \infty \quad (37)$$

Thus W^0 of Eq. (33) is dominated by the core region, and a numerical calculation is necessary to determine its dependence on d and ξ . We use a fit to the numerical computation for the antipodal vortex pair on a sphere, which yields,

$$W_{\text{sphere}}^0(\mathbf{d}, R) = \pi n_0 d^2 (1 + \mathcal{O}(\xi/R)). \quad (38)$$

It is possible to obtain analytically the far field contributions to the *determinant* exponent W^1 . Using (34,35) for each block l , yields

$$\begin{aligned} W^1 &= -\log |D_{12}/D_{11}| \\ &\simeq \sum_{l(\text{far})} \sum_{\mathbf{k}} \text{Re} \ln \left(\frac{1 - e^{i2(\phi_{2,l}-\phi_{1,l})} |Q_{\mathbf{k}}|^2}{1 - |Q_{\mathbf{k}}|^2} \right) \\ &\simeq \sum_{\mathbf{k}} \left(\frac{|Q_{\mathbf{k}}|^2}{1 - |Q_{\mathbf{k}}|^2} \right) \sum_{l(\text{far})} \text{Re} (1 - e^{2i(\phi_{2,l}-\phi_{1,l})}) \\ &= \delta n \int_{r_0} d^2x (1 - \cos(2\mathbf{d} \cdot \nabla \phi)) \\ &\simeq 2\pi \delta n d^2 \log(R/r_0), \end{aligned} \quad (39)$$

with $\delta n = 1/4\pi\xi^2$. Thus we find that the determinant diverges logarithmically with the size of the system, but with a coefficient that is of order δn and not n_0 .

A numerical computation was carried out for the Bogoliubov eigenvectors and the exact overlap exponent of an antipodal vortex pair on the sphere, as detailed in Appendix B. We used a set of coherence lengths in the

range $\xi/R \in [0.075, 0.15]$, and upper angular momentum cut-off $l_{\text{max}} = 60$. The fit to the numerical computation for W^0 of Eq. (32) is shown in Fig.6, where the data collapses onto the curve

$$W_{\text{sphere}}^0(\mathbf{d}, R) = \pi n_0 d^2 (1 + \mathcal{O}(\xi/R)) \quad (40)$$

Note that in contrast to the mean field theory (13), W^0 is finite in the thermodynamic limit.

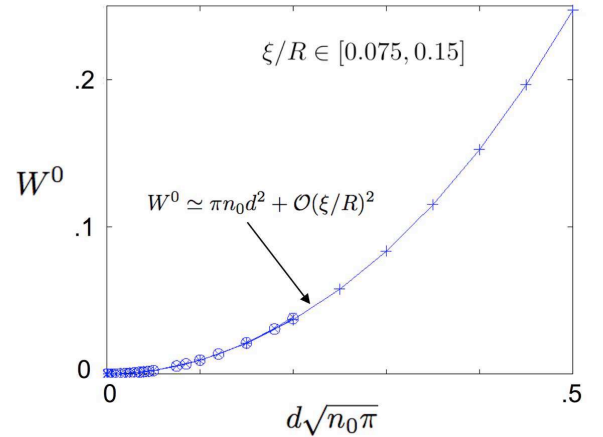


FIG. 6: The leading order overlap exponent for an antipodal vortex pair of a BEC on a sphere, displaced by a distance d . n_0 is the mean field condensate density. Numerical data for Eq. (32) are marked by crosses and circles representing different coherence lengths in the range $\xi/R \in [0.075, 0.15]$. The upper angular momenta cut-off was taken at $l_{\text{max}} = 60$. The solid line represents the asymptotic equation. Note that the leading order exponent has no logarithmic divergence with R , in contrast to the fluctuation correction W^1 , in Eq. (41).

The numerical calculation of the next order (prefactor)

contribution is shown in Fig.7, which yields

$$\begin{aligned} W_{\text{sphere}}^1 &= A(d, \xi) \log(CR/\xi) \\ A &\sim (d/\xi)^2 + \mathcal{O}(\xi/R)^2 \\ C &\simeq 0.33 \pm 0.01. \end{aligned} \quad (41)$$

These results can be used to extract the overlap exponent of a single vortex in the plane by halving expressions (40,41) and taking the large R limit, which gives

$$W = \frac{1}{2}\pi n_0 d^2 + 2\pi\delta n d^2 \log(CR/\xi). \quad (42)$$

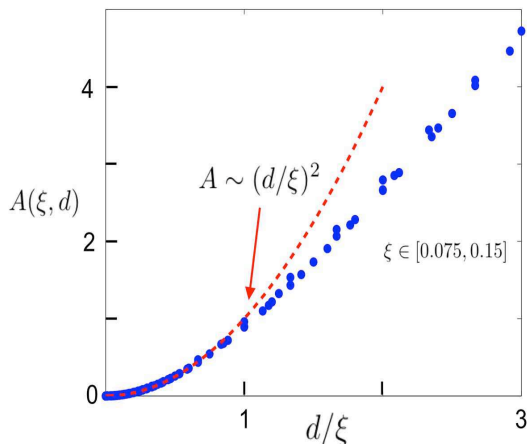


FIG. 7: The coefficient $A(d, \xi)$ of the fluctuations correction W^1 for the same systems as in Fig. 6. Note that the data collapse indicates that at large R/ξ , A depends only on the ratio d/ξ . $W^1(d, R)$ in Eq.(41) diverges logarithmically with R , which is an orthogonality catastrophe.

IV. VORTEX OVERLAP IN BCS STATES

We begin with a simple model for attractively interacting fermions, with a pairing instability:

$$\mathcal{H} = \int d^2x \left\{ \psi_s^\dagger (K + V) \psi_s - \frac{g}{2} \psi_s^\dagger \psi_{s'}^\dagger \psi_{s'} \psi_s \right\}$$

where $\psi_s(\mathbf{x})$ creates an electron of mass m , charge q and spin $s = \uparrow, \downarrow$ at position \mathbf{x} , and the operators of kinetic (K) and potential (V) energy are the same as defined for bosons in (15,14). Summation over repeated spin indices s, s' is assumed. The complex superconducting order parameter is $\varphi(\mathbf{x}) = \langle \psi_\uparrow(\mathbf{x}) \psi_\downarrow(\mathbf{x}) \rangle$. At long distances from the edges or vortex cores, φ minimizes the Ginzburg-Landau energy, i.e. it satisfies Gross Pitaevskii equation (17) with pair mass $2m$ and charge $q = 2e$. Its magnitude is given by the BCS gap parameter, i.e. $\Delta = g|\varphi|$.

As for the BEC, in the presence of a weak magnetic field, a quantized vortex solution minimizes the mean field energy, and its core size is given by the coherence length $\xi \simeq \hbar v_F / \pi \Delta_0$, where v_F is the Fermi velocity[3].

The Bogoliubov de-Gennes (BdG) equations for the superconductor are

$$\begin{aligned} H_0 U_n(\mathbf{x}) + g\varphi V_n(\mathbf{x}) &= E_n U_n(\mathbf{x}) \\ g\varphi^* V_n(\mathbf{x}) - H_0^* U_n(\mathbf{x}) &= E_n V_n(\mathbf{x}), \end{aligned}$$

where $H_0 = K - \mu$ and $\mu = \hbar^2 k_F^2 / 2m$, along with the self consistency condition,

$$\sum_n U_n(\mathbf{x}) V_n^*(\mathbf{x}) = \varphi(\mathbf{x}). \quad (43)$$

The self consistency determines the detailed profile of $|\varphi(\mathbf{r})|$ in the core region.

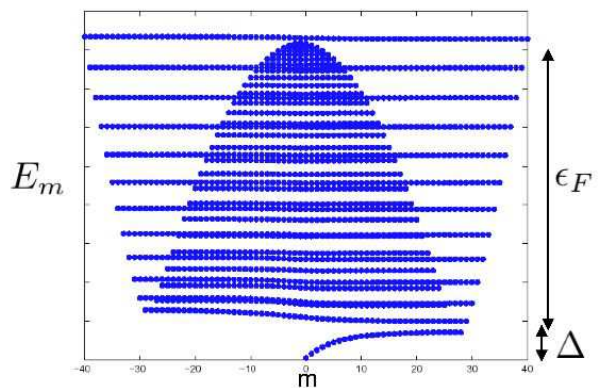


FIG. 8: The Bogoliubov-de Gennes spectrum for a vortex pair configuration on the sphere, as a function of azimuthal quantum number m . The relevant parameters are the BCS gap Δ , and the Fermi energy ϵ_F . Note the branch of (doubly degenerate) low energy Caroli-de Gennes-Matricon core states at positive angular momenta.

A. BCS vortex overlap

Using the solutions of (43) the vortex ground state is given by

$$\begin{aligned} |\Phi_0\rangle &= \mathcal{N} \exp\left(\psi_\uparrow^\dagger Q \psi_\downarrow^\dagger\right) |0\rangle \\ Q &= \langle \mathbf{x} | (U^\dagger)^{-1} V^\dagger | \mathbf{x}' \rangle, \end{aligned} \quad (44)$$

where \mathcal{N} is the normalization. The normalized overlap of two BCS vortex states displaced by \mathbf{d} is given by

$$e^{-W(d)} = \left| \det \left(U_1^\dagger U_2 + V_1^\dagger V_2 \right) \right|. \quad (45)$$

We first calculate the far field contribution, and see that it exhibits from a similar logarithmic divergence as the boson mean field wavefunctions. Asymptotically far from the cores, whose sizes are of given by ξ , one can diagonalize (43) using a constant order parameter $\varphi_i = \Delta e^{i\phi}$. The solution of (43) yields

$$U_{\mathbf{k}}^2 = \frac{1}{2} \left(1 + \frac{\zeta_{\mathbf{k}}}{\sqrt{\zeta_{\mathbf{k}}^2 + \Delta^2}} \right) \quad (46)$$

$$V_{\mathbf{k}}^2 = \frac{1}{2} \left(1 - \frac{\zeta_{\mathbf{k}}}{\sqrt{\zeta_{\mathbf{k}}^2 + \Delta^2}} \right) e^{i2\phi} \quad (47)$$

with $\zeta_{\mathbf{k}} = \hbar^2(k^2 - k_F^2)/2m$. Factorizing the determinant into blocks, as shown in Fig. 1, we obtain

$$W = W_{\text{core}} + \sum_{r_l > r_0} A_l w_l^{\text{far}}$$

$$w_l^{\text{far}} \simeq [(1 - \cos(\phi_{1,l} - \phi_{2,l}))] \int \frac{d^2k}{(2\pi)^2} U_{\mathbf{k}}^2 V_{\mathbf{k}}^2$$

$$W \simeq \frac{1}{2}\pi n_{\text{eff}} d^2 \ln(R/r_0) + W_{\text{core}}, \quad (48)$$

where $n_{\text{eff}} = k_F/4\pi\xi < n_e$.

The finite (but large) contribution of the core region requires a full diagonalization of the BdG equations. For the antipodal vortex pair on the sphere, the details of the computation are found in Appendix B. A fit to the numerically obtained values of W in Eq. (45) yields the asymptotic expressions at large R/d

$$W^{\text{BCS}} \simeq d^2 \left(\frac{k_F}{8\xi} \ln(R/\xi) + k_F^2 F(k_F\xi) \right) + \mathcal{O}(d^4) \quad (49)$$

where F is a dimensionless function of order 0.2, of the scaling variable $(k_F\xi)$ as demonstrated by the collapse of the numerical data for W in Fig. (9).

By (49) we can conclude that in the weak coupling BCS superconductor, the (finite) core contribution, which is of order $(k_F d)^2$ is non divergent, but large in magnitude. This effectively suppresses tunneling between pinning sites separated by more than a few Fermi wavelengths.

V. TRANSPORT THEORY

Motion of vortices, and the associated development of an electromotive force (EMF) across the system, is severely restricted below the superfluid transition, because of pinning by a disorder potential enforced by interactions between vortices. Thermally activated hopping produces a low temperature magnetoresistance [5, 6]

$$\frac{\partial R}{\partial B}^{\text{act}} = R_B^N e^{-U_b/(k_B T)} \quad (50)$$

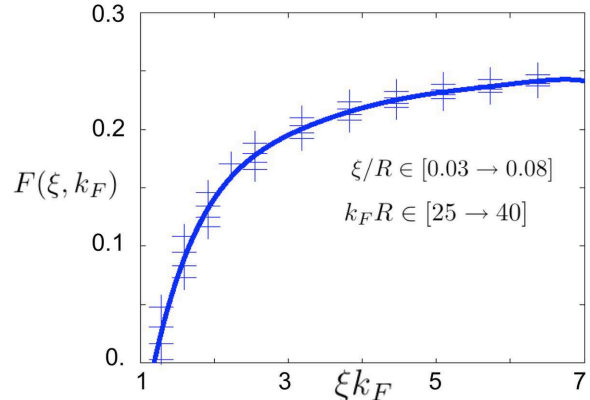


FIG. 9: The function $F(k_F, \xi)$ defined in Eq.(49), which yields the coefficient of the core contribution to the BCS vortex overlap on the sphere. k_F is the Fermi wavevector and ξ is Pipard's coherence length. The numerical data in the specified ranges of $k_F R$ and ξ/R , collapse to a function of the product ξk_F .

where R_B^N is of the order the normal state resistance divided by the upper critical field B_{c2} , and U_b is a typical energy barrier for vortex motion, which is of the order of the pinning potential \bar{V} . As temperature is lowered vortex quantum motion may become dominant. In weak coupling BCS superconductors, the core contribution to (49) effectively suppresses any 'single-shot' vortex tunneling events at a distance larger than a few Fermi wavelengths. Vortices could still be pushed by the bias current at low temperatures (of the order of core state energy spacing [31]), by the Bardeen-Stephen flux creep [6]. This 'frictional' motion involves impurity scattering inside the BCS vortex core [8], and we shall not discuss it in the following.

Is there hope to observe real quantum tunneling at experimentally accessible temperatures? The answer is yes, for a Bose condensate with low enough superfluid density. Vortices have been created in cold atom BEC's [32], and although they are neutral condensates, mass transport measurements could be designed by inducing pinning sites and a potential gradient, and watching the vortex motion. Below we shall calculate variationally the vortex tunneling rate for the BEC, and use it to deduce the dissipative transport coefficient.

In superconductor vortex motion effects charge transport, which can be measured by external leads. The realization of 'bosonic' superconductors might be found in underdoped cuprate superconducting thin films, whose superfluid density is known to vanish [33] with doping, and whose coherence length is short. Another possibility is a two dimensional array of low capacitance Josephson junctions, although we have not considered here the effects of the discrete lattice periodicity.

We emphasize that applying a simple BEC theory for cuprate superconductors is highly questionable – for example the underlying lattice structure and the d -wave nodal quasiparticles are not at all treated here. Nevertheless, this generic feature of vortex tunneling might be detected in a power law current-voltage characteristics.

A. Variational evaluation of the BEC tunneling rate

In the limit of weak disorder, and at low external magnetic field, the dissipative transport is a measure of single

$$\gamma = \frac{\pi}{\hbar} \bar{V}^2 \text{Im} \int \mathcal{D}[\eta, \eta^*, \eta', \eta'^*] \langle \Psi_1^0 | \tilde{\varphi}_2 + \eta \rangle G(\boldsymbol{\eta}, \boldsymbol{\eta}'; E_{\text{bias}}) \langle \tilde{\varphi}_2 + \eta' | \Psi_1^0 \rangle$$

$$G(\boldsymbol{\eta}, \boldsymbol{\eta}', E) = \int_{-\infty}^{\infty} dt \exp \left(\sum_n \left(a_n^* a'_n e^{i\omega_n t} - \frac{1}{2} (|a_n|^2 + |a'_n|^2) \right) - iEt/\hbar \right), \quad (51)$$

where a_n is given in (25).

We shall evaluate the multidimensional integrals here by the saddle point approximation, writing

$$\gamma \simeq \frac{\pi}{\hbar} \bar{V}^2 A[\tilde{\eta}, \tilde{\eta}^*] e^{-2W[\tilde{\eta}, \tilde{\eta}^*]} \times \exp \left(\sum_n (e^{i\omega_n \tilde{t}} - 1) |\tilde{a}_n|^2 - iE_{\text{bias}} \tilde{t}/\hbar \right) \quad (52)$$

where the tilde indicates the saddle point value, and where A is the fluctuation determinant. Differentiating with respect to \tilde{t} yields

$$E_{\text{bias}} = \sum_n \hbar \omega_n |\tilde{a}_n|^2 e^{i\omega_n \tilde{t}}, \quad (53)$$

which can be solved by setting $\tilde{t} = 0$, and finding that the left hand side of (53) is simply the classical distortion energy $E_{\text{cl}}[\tilde{\eta}, \tilde{\eta}^*]$ about the relaxed vortex. Here we neglect the smaller quantum energy from the zero point fluctuations.

Thus, the saddle point is given by solving

$$\left. \frac{\delta W[\eta, \eta^*]}{\delta \eta} \right|_{\tilde{\eta}, \tilde{\eta}^*} = 0, \quad E_{\text{cl}}[\tilde{\eta}, \tilde{\eta}^*] = E_{\text{bias}}. \quad (54)$$

That is to say, the complex field distortion $\tilde{\eta}(E_{\text{bias}}, d)$ minimizes the overlap W , under the energy constraint (53). The fluctuation prefactor A in (53) is given by

$$A = \hbar^{-1} \left(\frac{2\pi}{\sum_n \omega_n^2 |\tilde{a}_n|^2} \right)^{1/2}. \quad (55)$$

Including the Gaussian fluctuations the final expression for the tunneling decay rate is given by

$$\gamma \simeq \frac{\pi}{\hbar} \bar{V}^2 A(E_{\text{bias}}, d) e^{-2W(E_{\text{bias}}, d)} \quad (56)$$

vortex mobility. At zero temperature we relate it to the incoherent tunneling rate γ , as given by Eq. (8). For weakly interacting bosons, the only gapless excitations $|\Psi_2^\alpha\rangle$ about the classical vortex are the Bogoliubov modes with dispersion ω_n . To evaluate (8) we use the coherent state representation, writing

While an explicit $\tilde{\eta}(\mathbf{x})$ is computed variationally in Appendix C, one can determine the power-law dependence of $\gamma(E_{\text{bias}})$ by dimensional arguments. Assuming that the difference between the two vortex states is confined within a region of length-scale $\bar{R} \gg d, \xi$. By symmetry, the distortion energy is at least a quadratic function of d/\bar{R} ,

$$\frac{E_{\text{bias}}}{K\varepsilon_0} = \left(\frac{d}{\bar{R}} \right)^2 + \mathcal{O}(d/\bar{R})^3 \quad (57)$$

where $\varepsilon_0 = \pi \hbar^2 n_0/m$ is the ‘core energy’ of the vortex, and K an as-yet unknown dimensionless constant of order unity. The logarithmic divergence of the overlap (2) with \bar{R} together with (57) implies that

$$W[\tilde{\eta}] \simeq W_0(d) + \frac{\pi}{4} n_{\text{eff}} d^2 \ln \left(\frac{E_{\text{bias}}}{K\varepsilon_0} \right) \quad (58)$$

$$A = \sqrt{\frac{2\pi \bar{R}}{\hbar c E_{\text{bias}}}} \simeq \left(\frac{2\pi d}{\hbar c_s K \varepsilon_0} \right)^{1/2} \left(\frac{E_{\text{bias}}}{K\varepsilon_0} \right)^{-3/4}$$

where n_{eff} is the coefficient of the logarithmic divergence in Eq. (2) and $c_s = \hbar/m\xi$ is the speed of sound. Thus, the variational tunneling rate as a function of bias energy is given by

$$\gamma \simeq \gamma_0(d) \left(\frac{E_{\text{bias}}}{K\varepsilon_0} \right)^{\frac{\pi}{2} n_{\text{eff}} d^2 - \frac{3}{4}}$$

$$\gamma_0 \sim \frac{\pi}{\hbar} \bar{V}^2 \left(\frac{2\pi d}{\hbar c_s K \varepsilon_0} \right)^{1/2} e^{-W_0(d)} \quad (59)$$

In Appendix C use the displaced vortex core (DVC) trial configuration for the condensate phase in the far field

region. We indeed confirm that Eqs. (57) and (59) are asymptotically valid at small E_{bias} . and compute the coefficient $K \approx 2.27$.

B. Current-Voltage Relation

Steady vortex motion can be driven by an imposed current which produces an energy gradient (Magnus force) perpendicular to the current. In contrast to earlier treatments of the vortex motion as continuously driven by the Magnus force [9, 34] (where the superfluid velocity is corrected for the vortex motion), here we consider the vortex motion as a diffusion process involving random hopping events between pinning sites. Let the number current density of bosons be \mathbf{j}_s , the energy bias between pinning sites separated by \mathbf{d} is

$$E_{\text{bias}} = 2\pi\hbar \hat{\mathbf{z}} \times \mathbf{j}_s \cdot \mathbf{d}, \quad (60)$$

and the Magnus force is thereby identified as $\mathbf{F}_M = -\partial E_{\text{bias}}/\partial \mathbf{d} = 2\pi\hbar \mathbf{j}_s \times \hat{\mathbf{z}}$.

Determining the vortex velocity yields the transport equation. For superfluids with vorticity density n_v , the chemical potential gradient is $\nabla\mu = 2\pi\hbar n_v \mathbf{V} \times \hat{\mathbf{z}}$, while for a superconductor, the electromotive (EMF) field is

$$\mathbf{E} = -c^{-1} \mathbf{V} \times \mathbf{B} \quad (61)$$

where c is the speed of light. In Fig. 10, the hopping process of a vortex between two pinning potentials is depicted, along with the vectors \mathbf{j}_s , \mathbf{F}_M , \mathbf{V} , and the induced EMF \mathbf{E} .

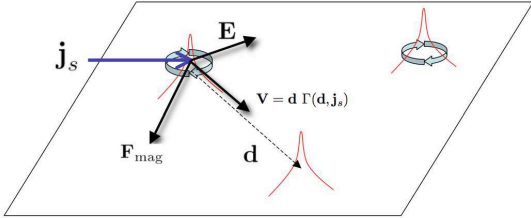


FIG. 10: The bias current \mathbf{j}_s , Magnus force \mathbf{F}_{mag} and induced electromotive field \mathbf{E} associated with hopping of a single vortex (marked by its circulating current) by a distance \mathbf{d} between pinning sites. The mean vortex velocity $\langle \mathbf{V} \rangle$ is calculated variationally in the text.

For an inhomogenous superconductor, with a random distribution $P_\ell(\mathbf{d})$ of distances between pinning sites, with a mean distance ℓ , the mean component of the velocity along \mathbf{F}_M , $V_{\parallel} \equiv \mathbf{V} \cdot \hat{\mathbf{F}}_M$, is dissipative. We assume that the distribution of distances $|\mathbf{d}|$ is highly peaked

about ℓ , and obtain

$$\langle V_{\parallel} \rangle = \int d^2d P_\ell(\mathbf{d}) \mathbf{d} \cdot \hat{\mathbf{F}}_M \gamma(\mathbf{d}, \mathbf{j}_s) \simeq \mathcal{B} \ell \gamma(\ell, j_s) \quad (62)$$

with $\mathcal{B} = \sqrt{\pi} \Gamma(\frac{1}{2} + \frac{1}{2}\alpha) / \Gamma(\frac{3}{2} + \frac{1}{2}\alpha)$, and where

$$\alpha = \pi n_{\text{eff}} \ell^2 - \frac{3}{4} \quad (63)$$

is the power law dependence of $\gamma(j)$ as given explicitly in Eq. (59).

Here, we shall not consider the Hall voltage [35] which is produced by a mean down- or up-stream vortex velocity (parallel to \mathbf{j}_s).

Combining Eqs. (59), (60), and (61) and adding the activated contribution, we obtain the full magnetoresistance as

$$\frac{\partial R}{\partial B} = R_B^N e^{-U_b/(k_B T)} + R_B^{\text{tunn}} \left(\frac{I}{I_c} \right)^{\alpha-1} \quad (64)$$

where

$$\begin{aligned} I_c &= \frac{eK\varepsilon_0}{2\pi\hbar\ell} L_y \simeq 2.94 I_{\text{cr}} \frac{\xi}{\ell} \\ R_B^{\text{tunn}} &= \frac{\alpha\mathcal{B}}{cI_c} \ell \gamma_0(\ell) L_x \\ &= C \frac{L_y}{L_x} \frac{\ell^2}{ec} \left(\frac{\bar{V}}{\varepsilon_0} \right)^2 (4\pi n_0 \ell \xi)^{1/2} e^{-W_0(\ell)} \end{aligned} \quad (65)$$

where L_x, L_y are a rectangular sample's dimensions, where I flows along the x direction. The characteristic current scale is of the order of $I_{r_{\text{mcr}}}$, the critical current of a thin film superconductor with order parameter density n_0 [36]. and

$$I_{\text{cr}} = \frac{4en_0}{3\sqrt{3}} \frac{\hbar}{m\xi} L_y \quad (66)$$

The characteristic magnetoresistance scale R_B^{tunn} is given by a dimensionless constant

$$C = \frac{2\pi^2\alpha\mathcal{B}}{\sqrt{2}K^{3/2}} \quad (67)$$

R_B^{tunn} is exponentially sensitive to the pinning length-scale through the parameter $W_0(\ell) \approx \pi n_0 \ell^2$ defined in (59). We can roughly estimate the dimensionful prefactor in (65) by taking $n_0 \approx n_{\text{eff}} \approx 1/(4\pi\xi^2)$, $\ell \approx \xi \approx 10^{-7}$ cm, and a moderate pinning potential $\bar{V} \approx \varepsilon_0$, which yields

$$R_B^{\text{tunn}} \simeq e^{-W_0(\ell)} \frac{L_x}{L_y} 50 [\Omega/\text{T}] \quad (68)$$

The vortex tunneling effects could be enhanced by increasing the geometrical anisotropy of the sample. As depicted schematically in Fig.(11), the power law α , associated with vortex tunneling, can be revealed by plotting the non linear magnetoresistance curves on a log-log plot, to extract the zero temperature asymptote.

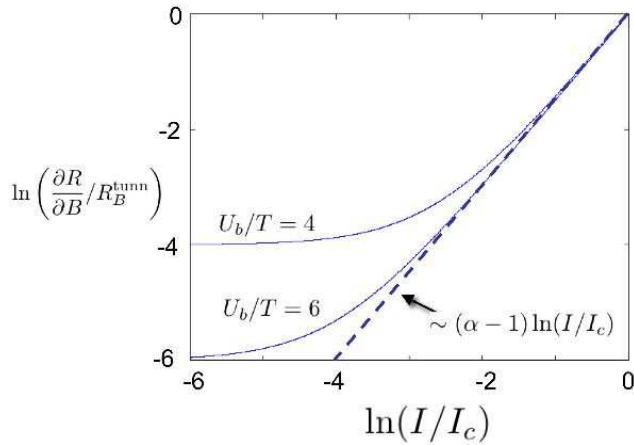


FIG. 11: A log-log plot of the zero field magnetoresistance of a two dimensional 'bosonic' superconductor (i.e. short coherence length, low superfluid density), as given by Eq. (64), with $R_B^N = R_B^{\text{tunn}}$. At finite temperatures, the low bias region is dominated by thermally activated magnetoresistance over barriers of height U_b . As temperature is reduced, vortex tunneling determines the asymptotic power law $I^{\alpha-1}$ where α is given by Eq.(63).

VI. VORTEX TUNNELING IN THE EFFECTIVE QUANTUM ELECTRODYNAMICS APPROACH

The quantum mechanical motion of a vortex results in the accrual of a geometric phase, given simply by $2\pi N_{\text{enc}}$, where N_{enc} is the number of bosons enclosed by the path of the vortex [37]. In a uniform condensate, leads to an effective vortex Lagrangian $L_0 = \pm 2\pi\hbar n_0 X\dot{Y}$, where n_0 is the boson density, and the sign follows the sign of the vorticity (assumed to be of unit strength).

Fluctuations in the bosonic background may be described by a linearized theory whose Lagrangian density resembles that of (2+1)-dimensional electrodynamics [4, 9, 38, 39, 40, 41], *viz.*

$$\mathcal{L} = -\frac{1}{4}mc^2 n_0 F_{\mu\nu} F^{\mu\nu} - 2\pi\hbar n_0 J^\mu (A_\mu + a_\mu), \quad (69)$$

where A_μ and $F_{\mu\nu}$ are gauge field and field strength tensor, and J^μ is the vortex 3-current. The dimensionless 'electric field' \mathbf{E} describes fluctuations in the boson current density: $\mathbf{E} = \hat{\mathbf{z}} \times \mathbf{j}/n_0 c$. The 'magnetic field' B describes fluctuations in the boson number density: $B = (n - n_0)/n_0$, and the background field is $b = \hat{\mathbf{z}} \cdot \nabla \times \mathbf{a} = 1$.

Integrating out the linearized phonons of the Bose fluid results in a complex, frequency-dependent vortex effective mass [18, 20, 22],

$$M_{\text{eff}}(\omega) \simeq \pi\xi^2 n_0 m \left\{ \ln\left(\frac{2c}{\omega\xi}\right) + \frac{1}{2}i\pi \text{sgn}(\omega) \right\}. \quad (70)$$

As shown in ref. [22], the motion of a vortex in an oscil-

ating superflow $\mathbf{v}_s(t)$ is described by

$$\mathbf{V}(\omega) = \frac{\mathbf{v}_s(\omega) + ir(\omega)\mathbf{v}_s(\omega) \times \hat{\mathbf{z}}}{1 - r^2(\omega)}, \quad (71)$$

where $r(\omega) = \omega M_{\text{eff}}(\omega)/2\pi\hbar n_0$. The vortex motion is therefore elliptically polarized, and at low frequencies, where $|r(\omega)| \ll 1$, the major axis is inclined at an angle $\theta_{\text{H}}(\omega) = \text{Im} r(\omega) = \pi|\omega|\xi/4c$ with respect to $\hat{\mathbf{z}} \times \mathbf{v}_s$. For the Ohmic case, $\theta_{\text{H}}(\omega)$ tends to a constant in the DC limit. The component of the vortex motion which lies along (and is in phase with) \mathbf{v}_s is then dissipative, and is associated with the radiation of phonons.

We have investigated the effects of this dissipation on vortex tunneling [35], and we find that the dissipation fails to localize the vortices. *I.e.* within this approach, vortices may enter into coherent superpositions. However, as we have shown here, such states are not possible due to the orthogonality catastrophe. This underscores an under-appreciated problem with the 'QED' theory of vortices, namely its inability to reproduce the orthogonality catastrophe. This, in turn, is due to the fact that the linearized electrodynamic theory (see *e.g.* ref. [22]) drops terms in \mathcal{L} which couple longitudinal and transverse degrees of freedom. A detailed discussion of this will be included in a forthcoming article [35].

VII. SUMMARY

In this paper we explored the relation between vortex motion in two-dimensional superfluids, and vortex wavefunction overlap. We found in Eq. (2) a vanishing of the overlap between mutually displaced vortices at any displacement, in the thermodynamic limit. This result is applicable to zero temperature (*i.e.* quantum) motion in the weak pinning and weak magnetic field regime. We find that the orthogonality catastrophe precludes the formation of extended vortex 'wavefunctions', such as Bloch waves.

The orthogonality catastrophe, however, does not necessarily eliminate incoherent (decay) tunneling in the presence of a bias current. The logarithmic divergence of the overlap exponent with system size has allowed us to variationally derive a power law relation between the tunneling probability and the bias current. This physics might be experimentally observable in angular momentum, or magnetization, relaxation, and in the non linear magnetoresistance of thin film superconductors at low temperature, provided the superfluid density and the mean distance between pinning sites are not too large. A tunneling induced magnetoresistance power law could be distinguished from other effects which involve multi-vortex interactions. For example: Anderson and Kim's [5] flux creep yields a voltage $V \sim e^{-F(I)/T}$, or Fisher's vortex glass phase has $V(I) \sim e^{-(I_c/I)^\mu}$ [42]. These multi-vortex effects would not approach, at low temperatures, the same straight line on a log-log plot as produced by incoherent vortex tunneling in Eq.(64).

In a future publication, we shall discuss the non dissipative (Hall) transport in terms of vortex tunneling and associated Magnus (Berry) phases [35].

VIII. ACKNOWLEDGEMENTS

We thank E. Altman, S. Gayen, A. Keren, D.-H. Lee, A. Mizel, E. Shimshoni, E. Sonin, Z. Tesanovic, and O. Vafek for helpful discussions. We gratefully acknowledge support from the US-Israel Binational Science Foundation and the hospitality of Aspen Center for Physics, Kavli Institute for Theoretical Physics and Technion Institute for Theoretical Physics, where portions of this research were carried out.

APPENDIX A: COHERENT STATE OVERLAP EXPONENT

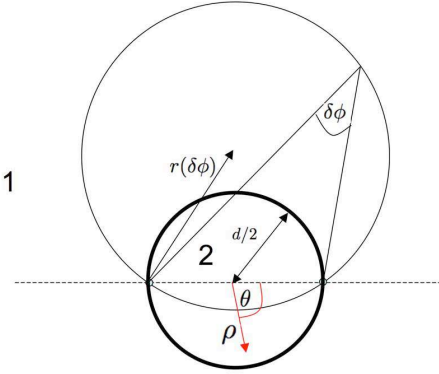


FIG. 12: Calculation of vortex coherent states overlap in Eq. (A1)

The real part of the overlap exponent between two coherent states displaced by a vector \mathbf{d} is given by Eq. (10). Let us take a simplified case of a core-less vortex with density n_0 on a two dimensional plane. We wish to evaluate the integral

$$W = n_0 \int_0^R dr r \int_0^{2\pi} d\theta (1 - \cos \delta\phi(r, \theta)) \quad (\text{A1})$$

where $\delta\phi = \phi(\mathbf{x} - \mathbf{d}/2) - \phi(\mathbf{x} + \mathbf{d}/2)$ is the phase shift due to the vortex motion. We separate the plane into two domains divided by circle of radius $d/2$ which passes through the two vortex centers as shown in Fig.12. In region 1, the loci of all points with $\delta\phi = \text{const}$ describes a circle of radius $r(\delta\phi) = d/2 \sin(\delta\phi)$. The portion of

the same circle inside region 2, has opposite values of $\cos(\delta\phi) \rightarrow -\cos(\delta\phi)$. Transforming the integration variable $\psi = \delta\phi$ leads to breaking up Eq. (A1) into

$$\begin{aligned} W &= n_0 (I_1 - I_2) \\ I_1 &= 4\pi \int_0^{\pi/2} d\psi r(\psi) \frac{dr(\psi)}{d\psi} (1 - \cos \psi) \\ I_2 &= 2 \int_{\text{region 2}} d^2x \cos \delta\phi \end{aligned} \quad (\text{A2})$$

which are evaluated as

$$\begin{aligned} I_1 &= \pi d^2 \int_{d/2R}^{\pi/2} d\psi \frac{\cos \psi}{(1 + \cos \psi) \sin \psi} \\ &= \frac{\pi}{2} d^2 (\ln(4R/d) - \frac{1}{2}) \\ I_2 &= d^2 \int_0^1 d\rho \rho \int_0^\pi d\theta \frac{1 - \rho^2}{\sqrt{(1 - \rho^2)^2 + 4\rho^2 \sin^2 \theta}} \\ &= d^2 (\frac{3}{4} - \frac{1}{2}G) \simeq 0.292 d^2 \end{aligned} \quad (\text{A3})$$

where $G = 0.91597\dots$ is the Catalan constant. Thus,

$$W = \frac{\pi}{2} n_0 d^2 \ln(2.014 R/d) \quad (\text{A4})$$

APPENDIX B: CALCULATIONS ON THE SPHERE

An antipodal vortex pair field can be expanded as

$$\varphi(\theta, \phi) = \sum_{l=1}^{\infty} \tilde{\varphi}_l Y_{l,1}(\theta, \phi) \quad (\text{B1})$$

where $Y_{lm}(\theta, \phi)$ are normalized spherical harmonics. Eq. (B1) is an eigenfunction of $L^z = -i\hbar \partial_\phi$. The coherence length ξ determines the core sizes at the north and south poles, and thus the the decay rate of the $\tilde{\varphi}_l$ with l .

The angular momentum representation, with a cut-off at $l_{\text{max}} \gg (R/\xi)$, reduces the Bogoliubov equations (23,43) to finite matrix diagonalizations. We can also translate the vortex wavefunctions using $SU(2)$ rotation $D_{mm'}^l$ matrices.

1. Bosonic State with Polar Vortex Pair

For the BEC vortex pair, some straightforward but tedious algebra, can bring the overlap exponent in Eq.

(32) into a computationally convenient form

$$\begin{aligned}
W^0 &= \text{Re} \left[(\varphi_1^* U_1 - \varphi_1 V_1) S_{12}^{-1} \right. \\
&\quad \left. \times (U_2^\dagger (\varphi_2 - \varphi_1) - V_2^\dagger (\varphi_2^* - \varphi_1^*)) \right] \\
W^1 &= \frac{1}{2} \ln \det[S_{12}] \\
S &= U_1^\dagger U_2 - V_1^\dagger V_2
\end{aligned} \tag{B2}$$

For the vortex pair field $\tilde{\varphi}$ given by (B1) the BdG equation possesses axial symmetry which allows $m = \bar{m}_n$ to be a good quantum number, and the BdG eigenvectors are

$$\begin{aligned}
U_{l,m}^n &= U_l^n \delta_{m,m_n}, \\
V_{l,m}^n &= V_l^n \delta_{m,m_n-2} \\
\delta_{nn'} &= \sum_l U_l^n U_l^{n'} - V_l^n V_l^{n'}
\end{aligned} \tag{B3}$$

for these coefficients is

$$\begin{aligned}
E_n \begin{pmatrix} U^n \\ -V^n \end{pmatrix} &= \begin{pmatrix} H^N & A \\ -A^\dagger & -H^N \end{pmatrix} \begin{pmatrix} U^n \\ -V^n \end{pmatrix} \\
H^N(m) &= \frac{\hbar^2}{2mR^2} l(l+1) \delta_{ll'} + V_{ll',m} \\
V_{ll',m} &= \langle l, m | V_{\text{pin}}(\theta) + 2g|\tilde{\varphi}|^2 - \mu | l', m \rangle \\
A_{ll'}(m) &= g \langle l, m | \tilde{\varphi}^2 | l', m-2 \rangle
\end{aligned} \tag{B4}$$

where (B8) can be used for the precise numerical evaluation of the matrix elements.

2. Boson Ground State Overlap

Having determined U_l^n, V_l^n , and recognizing that the transformation between φ_0, U_0, V_0 and φ_1, U_1, V_1 simply involves an $O(3)$ rotation of the z axis by an angle θ , the overlap (B2) is given by

$$\begin{aligned}
\langle \Phi_0 | \Phi_1 \rangle &= \det^{-1/2}[S] \exp[\tilde{\varphi}^\dagger I S^{-1} J \tilde{\varphi}] \\
S_{nn'} &= \sum_l \left(U_l^n D_{m_n, m_{n'}}^l U_l^{n'} - V_l^n D_{m_n, m_{n'}}^l V_l^{n'} \right) \\
I_{l,n} &= (U_l^n + V_l^n) \delta_{m_n, 1} \\
J_{n,l} &= U_l^n (\delta_{m_n, 1} - D_{m_n, 1}^l) + V_l^n (\delta_{m_n, 1} - D_{m_n-2, -1}^l) \\
\tilde{\varphi}_l &= \int d\Omega Y_{l,1}^*(\theta, \phi) \varphi(\theta, \phi).
\end{aligned} \tag{B6}$$

It is easy to verify that for the limit $U_l^n = \delta_{n,l}, V_l^n = 0$, (B6) reduces to the result for free particles.

3. Fermions on a Sphere

A polar vortex pair field described by Eq. (B1), defines the pairing order parameter

$$\Delta = \tilde{\varphi}(\theta, \phi) \tag{B7}$$

by normalizing it such that $\sqrt{n_0} = \Delta_0$. In the spherical harmonic basis $|l, m\rangle$ the Hamiltonian (43) simplifies greatly. The Laplacian is proportional to the diagonal operator \mathbf{L}^2 , and non diagonal matrix elements of functions $F(\theta, \phi)$ can be computed using $3j$ Racah coefficients [43]:

$$\begin{aligned}
&\langle l, m | F | l', m - M \rangle \\
&= \sum_{L,M} F_{LM} \left[\frac{(2l+1)(2L+1)(2l'+1)}{4\pi} \right]^{1/2} \\
&\quad \times (-1)^m \begin{pmatrix} l & L & l' \\ -m & M & m-M \end{pmatrix} \begin{pmatrix} l & L & l' \\ 0 & 0 & 0 \end{pmatrix} \\
F_{LM} &\equiv \int d\Omega Y_{L,M}^*(\Omega) F(\Omega)
\end{aligned} \tag{B8}$$

Due to axial symmetry, m is a good quantum number, which is to say that a function m_n is defined such that

$$\begin{aligned}
U_{l,m}^n &= U_l^n \delta_{m,m_n}, \\
V_{l,m}^n &= V_l^n \delta_{m',m_n-1}
\end{aligned} \tag{B9}$$

The matrix BdG equation for these coefficients is

$$\begin{aligned}
E_n \begin{pmatrix} U^n \\ V^n \end{pmatrix} &= \begin{pmatrix} H^N & A \\ A^\dagger & -H^N \end{pmatrix} \begin{pmatrix} U^n \\ V^n \end{pmatrix} \\
H^N &= \left(\frac{\hbar^2}{2mR^2} l(l+1) - \varepsilon_F \right) \delta_{ll'} \\
A_{ll'}(m) &= \langle l, m | \tilde{\varphi} | l', m-1 \rangle
\end{aligned} \tag{B10}$$

The overlap of two vortex pair states relatively rotated by θ is

$$\langle \Phi_0 | \Phi_1 \rangle = \det_{nn'} \left[\sum_l \left(U_l^n D_{m_n, m_{n'}}^l U_l^{n'} + V_l^n D_{m_n-1, m_{n'}-1}^l V_l^{n'} \right) \right] \tag{B11}$$

where $D_{mm'}^l(\theta)$ is the orthogonal rotation matrix.

APPENDIX C: VARIATIONAL TUNNELING RATE OF THE DISPLACED VORTEX CORE STATES.

Due to the orthogonality catastrophe, there is no wavefunction overlap between displaced ‘native’ (*i.e.* relaxed) vortices. This would seem to preclude vortex tunneling entirely, and would thereby have profound consequences for the particulate theory of vortices.

However, since it is only the vortex core whose position is determined by the potential, it is sensible to consider deformed vortex configurations in which the core is localized at a displaced position \mathbf{d} , but the far field flow configuration is centered elsewhere. This is the configuration which we seek in Eq.(54), in order to maximize the vortex overlap at constant energy bias E_{bias} . To this end,

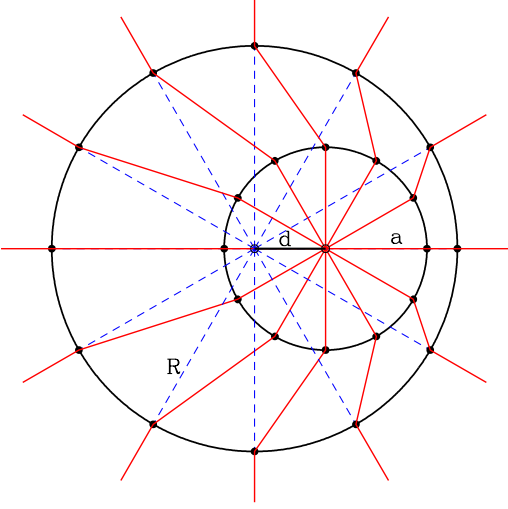


FIG. 13: The displaced vortex core (DVC) configuration. For $|\mathbf{x}| > R$, and for $|\mathbf{x} - \mathbf{d}| < a$, the coherent boson field $\varphi_{\text{DVC}}(\mathbf{x})$ corresponds to a native vortex centered at $\mathbf{x} = 0$ and $\mathbf{x} = \mathbf{d}$, respectively. In between, $\varphi_{\text{DVC}}(\mathbf{x})$ interpolates continuously.

consider the displaced vortex core (DVC) configuration depicted in Fig. 13. Let $\varphi_i(\mathbf{x})$, $i = 1, 2$ denote the vortex field centered at the origin, and at $\mathbf{x} = \mathbf{d}$, respectively. Let us ignore the core region and set $\varphi_1 \simeq \sqrt{n_0} \exp(i\phi_0)$,

We define the DVC state $\varphi_{\text{DVC}}(\mathbf{x}; \mathbf{d})$ as follows: Outside the circle $|\mathbf{x}| > R$, the configuration corresponds to a ‘native’ vortex centered at $\mathbf{x} = 0$, and the far phase field is $\phi = \phi_1$. Inside the inner circle, $|\mathbf{x} - \mathbf{d}| < a$ (with $d + a \leq R$), the DVC phase field $\phi = \phi_2$ is that of the native vortex centered at $\mathbf{x} = \mathbf{d}$. Between the two circles, we interpolate continuously between ϕ_1 and ϕ_2 in the outer and inner circles. Note that $\varphi_{\text{DVC}}(\mathbf{x}; \mathbf{0}) = \varphi_0(\mathbf{x})$. To simplify matters further, we assume $\xi \ll a$, and take and we interpolate by assuming lines of constant phase ϕ_{DVC} joining the circles $|\mathbf{x} - \mathbf{d}| = a$ and $|\mathbf{x}| = R$.

Due to the disturbance in the flow field $\mathbf{v} = \frac{\hbar}{m} \nabla \phi$, the DVC state has greater kinetic energy than the native vortex. This energy difference is found to be

$$\Delta = \varepsilon_0 \ln \left(\frac{R}{a} \right) \cdot \left\{ 1 - \sqrt{1 - \left(\frac{d}{R-a} \right)^2} \right\}, \quad (\text{C1})$$

where $\varepsilon_0 = \pi \hbar^2 n_0 / m$ is the ‘core energy’ of the vortex.

The far field contribution to the overlap in γ is

$$W_{\text{far}} = n_{\text{eff}} \int^R d^2x (1 - \cos(\phi_0 - \phi_{\text{DVC}})) \quad (\text{C2})$$

Dimensionally, one has $W = n_{\text{eff}} d^2 f(a/R, d/R)$.

Incoherent tunneling is dissipative; in a superfluid with mass current \mathbf{j}_s a vortex of unit strength feels a potential

$U(\mathbf{X}) = \kappa \hat{\mathbf{z}} \times \mathbf{j}_s \cdot \mathbf{X}$, where $\kappa = \hbar/m$ is the quantum of vorticity. A vortex tunneling a distance d between pinning sites can therefore avoid the orthogonality catastrophe by tunneling into a higher energy state with a displaced vortex core. The energy difference is supplied by the superflow, provided $d_{\perp} = \mathbf{d} \cdot \hat{\mathbf{z}} \times \mathbf{j}_s > 0$. The relative energy of the DVC state is thus fixed by the tunneling distance at $E_{\text{bias}} = \kappa j_s d_{\perp}$. If we fix E_{bias} , we may solve Eq. C1 to obtain

$$\frac{d}{R} = \left(1 - \frac{a}{R} \right) \sqrt{2\beta(1-\beta)} \quad ; \quad \beta = \frac{E_{\text{bias}}/\varepsilon_0}{\ln(R/a)}. \quad (\text{C3})$$

The variational part of the overlap exponent may then be written as $W = \frac{\pi}{2} n_{\text{eff}} d^2 h(a/R, E_{\text{bias}}/\varepsilon_0)$. Since a/R is a free parameter, we minimize W with respect to it, in order to maximize the tunneling amplitude. This yields an optimal value $W_{\text{opt}}(d, E_{\text{bias}}) = \frac{\pi}{2} n_0 d^2 g(E_{\text{bias}}/\varepsilon_0)$. Note that the energy E_{bias} depends only on the transverse part d_{\perp} of the tunneling displacement, and that

$$\frac{E_{\text{bias}}}{\varepsilon_0} = \frac{v_s}{c} \cdot \frac{2d_{\perp}}{\xi}, \quad (\text{C4})$$

where v_s is the velocity of the superflow.

In Fig. 14 we plot the function $g(E_{\text{bias}}/\varepsilon)$. For $E_{\text{bias}} \lesssim 0.1 \varepsilon_0$, we find

$$\begin{aligned} g &\simeq 0.41 - 0.50 \ln \left(\frac{E_{\text{bias}}}{\varepsilon_0} \right) \\ &\simeq -0.50 \ln \left(\frac{E_{\text{bias}}}{K\varepsilon_0} \right), \end{aligned} \quad (\text{C5})$$

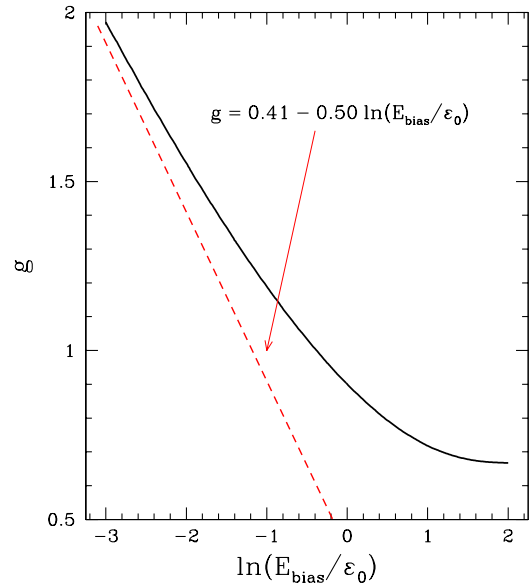


FIG. 14: Solid line: The overlap exponent function g as a function of the bias energy E_{bias} and core energy ε_0 . Dashed line: a logarithmic function which appears to be a viable asymptotic limit at low bias.

with $K \approx 2.27$. Thus, we obtain

$$e^{-W_{\text{opt}}(d, E_{\text{bias}})} \simeq \left(\frac{E_{\text{bias}}}{K \varepsilon_0} \right)^{\pi n_{\text{eff}} d^2 / 4}. \quad (\text{C6})$$

Thus we find that the variational calculation confirms

the dimensional arguments leading to (57) and (59) and the power law tunneling rate $\gamma(E_{\text{bias}})$ in (59). As the energy E_{bias} increases, we find that g flattens out, and for $E_{\text{bias}} \gtrsim 10 \varepsilon_0$ we find $g \approx 0.67$.

-
- [1] V.L. Berezinskii, *Sov. Phys.-JETP* **32**, 493, (1970); J.M. Kosterlitz and D.J. Thouless, *Phys. C: Solid St. Phys.* **5** 1246 (1972).
- [2] P. W. Anderson, *Rev. Mod. Phys.* **38**, 298 (1966).
- [3] M. Tinkham, *Introduction to Superconductivity*, (Krieger, NY (1980)).
- [4] V. Ambegaokar *et al.*, *Phys. Rev. B* **21**, 1806 (1980).
- [5] P. W. Anderson and Y. B. Kim, *Rev. Mod. Phys.* **36**, 39 (1964).
- [6] J. Bardeen and M. J. Stephen, *Phys. Rev.* **140**, 1197 (1965).
- [7] M. V. Feigel'man *et al.*, *Sov. Phys. JETP* **5**, 711 (1993) (*Pis'ma Eksp. Teor. Fiz.* **57**, 699 (1993)); G. Blatter *et al.*, *Rev. Mod. Phys.* **66**, 1125 (1994); A. van Otterlo, M. Feigel'man, V. Geshkenbein, and G. Blatter, *Phys. Rev. Lett.* **75**, 3736 (1995).
- [8] N. B. Kopnin, *Rep. Prog. Phys.* **65**, 1633 (2002).
- [9] G. Volovik, *JETP Lett.* **62**, 65 (1995).
- [10] G. Blatter, V. B. Geshkenbein and V. M. Vinokur, *Phys. Rev. Lett.* **66** 3297 (1991); P. Ao and D. J. Thouless, *Phys. Rev. Lett.* **70**, 2158 (1993); M. J. Stephen, *Phys. Rev. Lett.* **72**, 1534 (1994).
- [11] A. J. J. van Dalen, *et al.*, *Phys. Rev. B* **54** 1366, (1996).
- [12] D. Ephron, A. Yazdani, A. Kapitulnik, and M. R. Beasley, *Phys. Rev. Lett.* **76**, 1529-1532 (1996); J. B. Majer, J. Peguiron, M. Grifoni, M. Tsuveland and J. E. Mooij, eprint cond-mat/0301073.
- [13] Q. Niu, P. Ao and D. J. Thouless, *Phys. Rev. Lett.* **72**, 1706 (1994); J.-M. Duan, *Phys. Rev. Lett.* **75**, 974 (1995) [C]; Q. Niu, P. Ao, and D. J. Thouless, *Phys. Rev. Lett.* **75**, 975 (1995)[C].
- [14] E. B. Sonin, *Sov. Phys. JETP* **37**, 494 (1974); (*Zh. Eksp. Teor. Fiz.* **64**, 970 (1973)); E. B. Sonin, *Physica B* **210**, 234 (1995).
- [15] This approach has been used to calculate tunneling rates of fractionally charged quasiparticles in the Quantum Hall phase: A. Auerbach, *Phys. Rev. Lett.* **80**, 817 (1998); E. Shopen, Y. Gefen, Y. Meir, cond-mat/0503608.
- [16] A. Mizel, cond-mat/0107530.
- [17] P. Nozières and C. de Dominicis, *Phys. Rev.* **178**, 1097 (1969); G. Yuval and P. W. Anderson, *Phys. Rev. B* **1**, 1522 (1970) ; P. W. Anderson, G. Yuval, and D. R. Hamann, *Phys. Rev. B* **1**, 4464 (1976).
- [18] R. P. Feynman and F. L. Vernon, Jr., *Ann. Phys. (N.Y.)* **24**, 118 (1963); A. O. Caldeira and A. J. Leggett, *Ann. Phys.* **149**, 347 (1983); U. Weiss, *Quantum Dissipative Systems* (World Scientific, Singapore, 1993).
- [19] S. Chakravarty, *Phys. Rev. Lett.* **49**, 681 (1982).
- [20] U. Eckern and A. Schmid, *Phys. Rev. B* **39**, 6441 (1989); U. Eckern and E. B. Sonin, *Phys. Rev. B* **47**, 505 (1993). R. Fazio, A. van Otterlo, and G. Schön, *Europhys. Lett.* **25**, 453 (1994); R. Iengo and G. Jug, *Phys. Rev. B* **52**, 7536 (1995).
- [21] J. Duan, *Phys. Rev. B* **48**, 333 (1993); *ibid.* **49**, 12381 (1994).
- [22] D. P. Arovas and J. A. Freire, *Phys. Rev. B* **55**, 1068 (1997).
- [23] A standard example of Heitler-London approach can be found in D.C. Mattis, 'Theory of Magnetism I', (Springer-Verlag, 1988) Ch 2.2.
- [24] E. P. Gross, *Nuovo Cimento* **20**, 454 (1961).
- [25] L. P. Pitaevskii, *Zh. Eksp. Teor. Fys.* **40**, 646 ; [*Sov. Phys. JETP*, **13**, 451] (1961).
- [26] For example see: A. L. Fetter and A. S. Svidzinsky, *J. Phys. Cond. Matt* **13**, R135 (2001); S. Ghosh, *Phase Transitions* **77**, 625 (2004).
- [27] C. Pethick and H. Smith, *Bose-Einstein Condensation in Dilute Gases* (Cambridge University Press, Cambridge (2002)), Ch. 9.
- [28] M. Edwards *et al.*, *J. Res. Natl. Inst. Stand. Techol.* **101**, 553 (1996); A. Fetter, *Phys. Rev. A* **53**, 4245 (1996);
- [29] Y. Castin, in *Coherent atomic matter waves*, Lecture Notes of Les Houches Summer School, edited by R. Kaiser, C. Westbrook, and F. David, EDP Sciences and Springer-Verlag (2001).
- [30] J. Steinhauer *et al.*, *Phys. Rev. Lett* **88**, 120407 (2002); J. Steinhauer *et al.*, *Phys. Rev. Lett* **90**, 060404 (2003).
- [31] C. Caroli, C.; P.G. de Gennes and J. Matricon, *Phys. Lett.* **9** 307 (1964).
- [32] M.R. Mathews, *et al.*, *Phys. Rev. Lett.* **84**, 2498, (1999); (2001); K. W. Madison *et al.*, *Phys. Rev. Lett.* **84**, 806 (2000); J. R. Abo-Shaer, *et al.* *Science*, **292**, 476 (2001); E. Hodby, *et al.* *Phys. Rev. Lett.* **88**, 010405 (2002).
- [33] Y. J. Uemura *et al.*, *Phys. Rev. Lett* **62** 2317 (1989).
- [34] P. Nozieres and W.F. Vinen, *Philos. Mag.* **14**, 667 (1966); D. J. Thouless, Ping Ao, and Qian Niu, *Phys. Rev. Lett.* **76**, 3758 (1996); C. Wexler, *Phys. Rev. Lett.* **79**, 1321 (1997).
- [35] D. P. Arovas and A. Auerbach, in preparation.
- [36] P.G. de-Gennes, 'Superconductivity of Metals and Alloys', (Addison Wesley, 1964), Ch. 6-5.
- [37] D. P. Arovas, J. R. Schrieffer, and F. Wilczek, *Phys. Rev. Lett.* **53**, 722 (1984); F. D. M. Haldane and Y.-S. Wu, *ibid.* **55**, 2887 (1985); P. Ao and D. J. Thouless, *ibid.* **70**, 2158 (1993).
- [38] V. N. Popov, *Sov. Phys. JETP* **37**, 341 (1973).
- [39] M. P. A. Fisher and D.-H. Lee, *Phys. Rev. B* **39**, 2756 (1989).
- [40] A. Zee, *Nucl. Phys. B* **421**, 111 (1994).
- [41] E. Šimánek, *Inhomogeneous Superconductors* (Oxford University Press, Oxford, 1994).
- [42] M. P. A. Fisher, *Phys. Rev. Lett.* **62**, 1415 (1989).
- [43] A. R. Edmonds, *Angular Momentum in Quantum Mechanics* (Princeton University Press, Princeton, 1996).